

An HIV-1 encoded peptide mimics the DNA binding loop of NF- κ B and binds thioredoxin with high affinity

By: Guoping Su, Wang Min, and [Ethan Will Taylor](#)

Guoping Su, Wang Min, and Ethan Will Taylor. An HIV-1 encoded peptide mimics the DNA binding loop of NF- κ B and binds thioredoxin with high affinity. *Mutation Research/Fundamental and Molecular Mechanisms of Mutagenesis* Volume 579, Issues 1–2, 11 November 2005, Pages 133-148. <https://doi.org/10.1016/j.mrfmmm.2005.02.019>

***© 2005 Elsevier B.V. Reprinted with permission. This version of the document is not the version of record. ***



This work is licensed under a [Creative Commons Attribution-NonCommercial-NoDerivatives 4.0 International License](#).

Abstract:

Pro-fs is a human immunodeficiency virus type 1 (HIV-1)-encoded putative selenoprotein, predicted by a theoretical analysis of the viral genome; it is potentially expressed by a –1 frameshift from the protease coding region. Pro-fs has significant sequence similarity to the DNA binding loop of nuclear factor kappa B (NF- κ B), which is known to bind thioredoxin (Trx). We hypothesize that the putative HIV-1 *pro-fs* gene product functions by mimicry of NF- κ B via binding to Trx. The hypothesis was tested in vitro by co-immunoprecipitation and GST-pull down assays, using a purified mutant pro-fs protein, in which the two potential selenocysteine residues were mutated to cysteines, in order to permit expression in bacteria. Both experiments showed that pro-fs binds to human wild type Trx (Trx-wt) with high affinity. Mutation of the two conserved cysteine residues in the Trx active site redox center to serine (Ser) (Trx-CS) weakened but failed to abolish the interaction. In pro-fs-transfected 293T cells, using confocal microscopy and fluorescence resonance energy transfer (FRET), we have observed that pro-fs localizes in cell nuclei and forms oligomers. Upon stimulation by phorbol 12-myristate 13-acetate (PMA), Trx translocates into cell nuclei. Significant FRET efficiency was detected in the nuclei of PMA-stimulated 293T cells co-expressing fluorescence-tagged pro-fs and Trx-wt or Trx-CS. These results indicate that in living cells the double cysteine mutant of pro-fs binds to both Trx and Trx-CS with high affinity, suggesting that Trx-pro-fs binding is a structurally-specific interaction, involving more of the Trx molecule than just its active site cysteine residues. These results establish the capacity for functional mimicry of the Trx binding ability of the NF- κ B/Rel family of transcription factors by the putative HIV-1 pro-fs protein.

Keywords: HIV-1 protease | Nuclear factor kappa B (NF- κ B) | Thioredoxin | Selenoprotein | Frameshift

Article:

1. Introduction

Pro-fs is a human immunodeficiency virus type 1 (HIV-1)-encoded putative selenoprotein that was predicted by Taylor et al. based on a theoretical analysis of the viral genome; it is potentially expressed by a -1 frameshift from the protease coding region, and contains two in-frame UGA codons downstream of the frameshift site [1], [2]. UGA generally serves as a stop codon, but in both eukaryotic and prokaryotic selenoprotein genes, it can be recoded as a sense codon for selenocysteine (Sec, U in single letter amino acid code), the selenium (Se) analog of cysteine (Cys) [3], [4], [5]. The amino acid sequence of pro-fs is highly conserved in HIV-1 subtypes B and D, especially in the region spanning the UGA codons [6], [7], [8]. Sequence analysis suggested a match to the nuclear factor kappa B (NF- κ B)/Rel family of transcription factors of higher eukaryotes, in which the conserved amino acid Cys62 residue aligns with the first highly conserved UGA codon of pro-fs [7]. The frameshift site in the HIV-1 protease gene occurs just upstream of the pro-fs sequence RYRSRU, which is related to the sequence of the NF- κ B/Rel family DNA binding domain, RFRYXC [7], the peptide of NF- κ B that interacts with thioredoxin (Trx). The predicted frameshift was shown to be functional in a standard in vitro translational assay [7]. Sequence alignments suggest that the protease-processed form of pro-fs could be a minimal NF- κ B-like DNA-binding domain. Indeed, mammalian cells co-expressing pro-fs and a HIV-1 long terminal repeat (LTR)-*lacZ* reporter construct showed increased β -gal activity, and mutations of the NF- κ B binding sites located in the HIV LTR abolished the effect (Taylor et al, unpublished data). In addition, the same region of NF- κ B is also a direct target of Trx [7], [9].

HIV employs cellular transcription factors that interact with the promoter/enhancer region of the LTR to activate its replication. NF- κ B is now recognized as a key regulator of HIV replication [10], [11], [12], [13], [14], [15]. NF- κ B is composed of homo- or heterodimers of Rel family proteins (reviewed in [16]), which all share an N-terminal Rel homology domain (RHD) that is essential for DNA binding and dimerization. The classic NF- κ B heterodimer (p50/p65) is sequestered in the cytoplasm by interaction with the inhibitory molecule I κ B [16]. Initial activation of NF- κ B in the cytosol occurs with phosphorylation and degradation of I κ B, which results in unmasking of a nuclear translocation signal on NF- κ B. Then the free NF- κ B dimers can enter the nucleus and bind DNA to start gene transcription [17], [18], [19], [20], [21], [22]. There are two conserved κ B sites located in HIV LTR that are binding targets of NF- κ B. Thus, the DNA-binding activity of NF- κ B is a crucial factor in HIV replication.

Transcriptional activation of the HIV LTR via NF- κ B can be stimulated by a variety of proinflammatory or pathogenic stimuli including inflammatory cytokines, phorbol esters (PMA), T-cell mitogens, lipopolysaccharide, hydrogen peroxide (H₂O₂) and tumor necrosis factor alpha (TNF- α) [23], [24], [25], [26], which function at least in part by inducing reactive oxygen species (ROS). NF- κ B is susceptible to regulation by alterations in the intracellular reduction-oxidation (redox) state [14], [27]. Just as oxidants can activate NF- κ B, antioxidants, such as Se, *N*-acetylcysteine (NAC), and lipoic acid, can effectively suppress the activation of NF- κ B [24], [28], [29], [30], [31], [32], [33]. Se is an essential trace element important for various aspects of human health (reviewed in [34]). Its antioxidative function is associated with specific selenoproteins including glutathione peroxidase (GPx) and thioredoxin reductase (TR) in the form of Sec. Growing evidence links Se deficiency to the occurrence, virulence, or disease progression of several viral infections, such as HIV-1, Coxsackie virus, and hepatitis B and C viruses [35], [36], [37], [38], [39], [40], [41]. A statistically significant clinical correlation between HIV disease outcome and patient Se status has been widely documented [37], [38], [42].

Moreover, Se is also an independent predictor of mortality in HIV infection [35], [37], [39]. Se supplementation was shown to suppress HIV replication induced by TNF- α or interleukin 1 (IL-1) by increasing the synthesis and activity of cellular selenoproteins GPx and TR [31], [43], [44], [45].

Activation of NF- κ B has been shown to be susceptible to redox regulation by the selenoprotein TR and its substrate Trx. Mammalian TR has two redox-active centers. The N-terminal center, conserved in all species that encode TR, is formed by two Cys residues. The redox center in the C-terminus is found only in TR of mammals and *C. elegans*, and is formed by a conserved Cys residue and a conserved Sec residue [35], [36], [37], [38], [39], [40], [41]. This Sec is required for catalytic activity of mammalian TR, whose activity is therefore tightly regulated by dietary Se status [46], [47].

Trx is known to be an important endogenous redox-regulating molecule with thiol reducing activity [48], [49], [50]. Trx plays a role in modulating various kinds of gene expression. It is a small ubiquitous protein with two Cys residues in its catalytic center with the consensus amino acid sequence Trp-Cys-Gly-Pro-Cys-Lys. Trx participates in redox reactions by reversible oxidation of the dithiol of its Cys32 and Cys35 residues to an intramolecular disulfide bond by TR. It catalyzes dithiol-disulfide exchange reactions involving many thiol-dependent cellular processes, including intracellular signaling, gene regulation, resistance to oxidant stress, and control of apoptosis [50], [51], [52]. Hirota et al. demonstrated that Trx plays dual and opposing roles in the regulation of NF- κ B. Overexpression of wild-type Trx suppressed NF- κ B activation in the cytoplasm, while overexpression of nuclear-targeted Trx enhanced NF- κ B-dependent transcription in the nucleus [48]. It was shown that the conserved residue Cys62 in the NF- κ B RHD domain needs to be maintained in a reduced (thiol) state in order for NF- κ B to bind to DNA [27], [53], e.g., κ B sites in HIV LTR. A growing body of evidence shows that Trx serves as a reductive catalyst in the reduction reaction of the Cys62 residue of NF- κ B via direct association with the DNA binding loop of NF- κ B [27], [48], [53].

The general aim of this paper is to clarify how the putative HIV-1 protein, pro-fs, might regulate HIV gene replication via NF- κ B, and to elucidate a potential mechanistic role of pro-fs in cells, particularly in regard to possible interactions with Trx. We hypothesized that Trx is a target of pro-fs because of the local sequence similarity mentioned above, between a central region of pro-fs and the DNA binding loop of NF- κ B, which contains the critical Cys residue that must first be reduced by Trx in order for NF- κ B to bind to DNA. A homology model of pro-fs peptide binding to Trx was constructed and the minimized non-bonded interaction energy of this complex was shown to be at least as favorable as that of a model derived from the NMR structure of a Trx-NF- κ B complex (Taylor et al., unpublished data). Therefore, we investigated the potential protein-protein interaction between pro-fs and Trx using co-immunoprecipitation and GST-pull down assays in vitro. We also applied confocal fluorescence resonance energy transfer (FRET) microscopy to examine whether Trx and pro-fs interact in living mammalian cells. Our data demonstrate consistently that pro-fs binds to human wild type Trx (Trx-wt) with high affinity. The mutation of the two conserved Cys residues in the redox center of Trx to Ser (Trx-CS) failed to abolish the interaction both in vitro and in living cells, suggesting that Trx-pro-fs binding is a structurally specific interaction that involves multiple amino acid residues in the interactive region.

2. Materials and methods

2.1. Construction of HIV-1 *pro-fs* for bacterial expression

Because the hypothetical HIV-1 encoded peptide *pro-fs* was predicted to be expressed by a -1 frameshift from the protease coding region, and *pol* is also expressed via a -1 frameshift from the *gag* coding region [1], the primary gene product would be a gag-pol-*pro-fs* fusion protein of 557 amino acids (aa), with an expected molecular mass of about 62.3 kDa. Because the N-terminal of HIV protease is located immediately upstream of the frameshift site [1], the first 20 residues of *pro-fs* are identical to those of protease. Hence, the *pro-fs* protein, which is the C-terminal 69 aa of the predicted gag-pol-*pro-fs* fusion product, should be cleaved off by protease and released as an independent small protein (about 8.3 kDa), in which form it has significant sequence similarity to NF- κ B. It was this low molecular mass peptide that we have cloned. The above molecular mass was estimated using Protein Calculator (<http://www.scripps.edu/~cdputnam/protcalc.html>).

The full-length *pro-fs* gene was obtained by PCR from the constructs provided by Dr. Robert J. Hondal (University of Vermont), which was cloned from the BH10 strain of HIV-1. In this construct, the two in frame UGA codons were mutated to Cys codons for bacteria expression, since bacteria and mammals utilize different cellular machinery for selenoprotein production. The stop codon TAA was mutated back from CAA in the original construct by amplifying the *pro-fs* coding region using sense primer PROFS-BAM, 5-GAT ATC GGA TCC GTT CAA CTT CCC GC-3, containing a *Bam*HI site, and anti-sense primer PROFS-ECO, 5-AGC TCG AAT TCT TAT GTC CAC AGA TTT CTA TGA G-3, containing an *Eco*RI site. A protease site was constructed immediately before *pro-fs* coding region. The PCR product was then digested by *Bam*HI and *Eco*RI and inserted into vector pET43.1b (Novagen), which contains a Nus·Tag and a hexahistidine (6x His) tag upstream of the cloning site (Fig. 1). The *pro-fs* gene construct (Nus-*pro-fs*) was transformed into *Escherichia coli* (*E. coli*) strain BL21 (DE3) from Stratagene (La Jolla, CA) using chemical transformation method followed by extraction and purification using QIAprep Miniprep Kits (Qiagen). Fidelity of the construct was verified by automated DNA sequencing (Molecular Genetics Instrumentation Facility, University of Georgia).

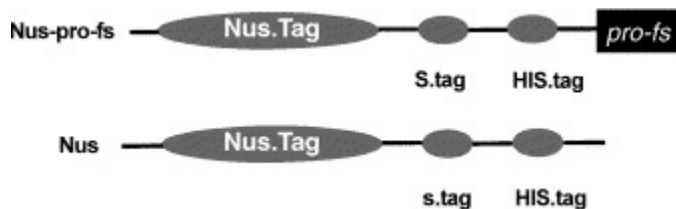


Fig. 1. Schematic structures of Nus-*pro-fs* and Nus proteins. *Pro-fs* was fused to the C-terminus of Nus·Tag as Nus-*pro-fs*. The vector alone expressed in *E. coli* BL21 (DE3), Nus protein, was used as negative control through out the studies. His·Tag in the fusion protein binds to HiTrap metal chelating column loaded with Ni₂SO₄ to enable purification using HPLC.

2.2. Production of Nus-*pro-fs* and Nus proteins in bacteria

The transformed bacteria were cultured in 50 ml of LB medium supplemented with 50 μ g/ml of Ampicillin for about 6 h at 37 $^{\circ}$ C with vigorous shaking until the optical density at 600 nm

(OD₆₀₀) was 0.6–1.0. This was stored overnight at 4 °C and was then used to infect 1 L of the same medium as described above on the next day. Isopropyl-β-d-thiogalactopyranoside (IPTG) (Fisher Scientific) was added to the bacterial culture to a final concentration of 0.5 mM when the OD₆₀₀ of culture reached 0.5 at 37 °C to induce protein production of Nus-pro-fs. The bacteria were continuously incubated with vigorous shaking at 30 °C for another 8 h before harvesting. The pET43.1b vector alone was transformed into *E. coli* BL21 (DE3) and Nus protein was produced using the protocol described above.

2.3. Protein purification using high performance liquid chromatography (HPLC)

Bacteria transformed with Nus-pro-fs construct or vector alone were harvested by centrifugation at 6000 × *g* for 30 min at 4 °C. Cell pellets were resuspended in buffer A (20 mM sodium phosphate, 0.5 M NaCl, pH 7.4) and cells were disrupted on ice by sonication using a model 550 Sonic Dismembrator (Fisher Scientific) in the presence of protease inhibitor (Roche). Cell debris and the soluble fraction in buffer A were then separated by centrifugation at 10,000 × *g* for 30 min at 4 °C. The supernatant was immediately loaded into a Äkta Purifier (Pharmacia Biotech) to be fractionated on a HiTrap™ metal chelating column (Amersham Biosciences) using HPLC. Proteins were eluted from the column by application of a linear gradient of 0–0.5 M imidazole in Buffer B (0.5 M imidazole, 20 mM sodium phosphate, 0.5 M NaCl, pH 7.4).

Protein concentrations of each fraction were determined with Bio-Rad protein assay solution and aliquots were analyzed in Western blots to detect Nus-pro-fs or Nus protein with mouse anti-Nus-Tag monoclonal antibody (Ab) (Novagen) and alkaline phosphatase (AP) conjugated goat anti-mouse-IgG secondary Ab. Signals were detected using Western Blue reagent (Promega) following the manufacture's instructions.

2.4. Co-immunoprecipitation and immunoblotting

For immunoprecipitation to analyze protein interaction *in vitro*, 3 μg of purified Nus-pro-fs and 5.5 μg of rabbit polyclonal anti-Trx Ab (Sigma) were mixed with or without 2 μg of human Trx (Sigma) and incubated for overnight at 4 °C on a 3D rotor. The mixture was then added to the Protein A magnetic beads (NEB) to incubate on 3D rotor for 2 h at 4 °C. Nus protein was used to incubate with Trx and Trx Ab for the same procedure as a negative control. The beads were separated from the supernatant by applying the mixture to the Dynal Magnetic Particle Concentrator (MPC, Dynal Biotech) for 2 min and followed with four washes with 1 ml of cold 0.1 M sodium phosphate buffer (pH 8.0). The immune complexes binding to the beads were eluted with 30 μl of cold 0.1 M glycine (pH 2.5) by gentle vortexing and inverting. Ten microlitres of the sample was analyzed in Western blots as described above.

2.5. GST-pull down assay

To elucidate whether the interaction between pro-fs and Trx is due to the intermolecular disulfide bonds between the Cys residues of pro-fs and the ones in Trx redox center, two GST-Trx fusion proteins were used for a GST-pull down assay to study their interactions. Wild-type GST-Trx fusion protein (GST-Trx-wt) and a mutant GST-Trx fusion protein (GST-Trx-CS), in

which the Cys32 and Cys35 residues in Trx redox center were mutated to Ser [49], were generously provided by Dr. Wang Min (Department of Pathology, Yale University School of Medicine, New Haven, CT). In brief, GST-Trx fusion proteins expressed in *E. coli* XL-1 blue were affinity purified on glutathione-Sepharose (GSH) beads (Pharmacia) [49]. Three micrograms of Nus-pro-fs were added to 50 μ l of GSH beads alone or 50 μ l beads bound with GST-Trx-wt or GST-Trx-CS. Fifty microlitres of cold 1X PBS buffer was added to each reaction to bring the final volume to 100 μ l. Three micrograms of Nus protein was incubated with GST-Trx-wt or GST-Trx-CS using the same procedure as negative controls. After overnight incubation at 4 °C on 3D rotor, the beads were separated from supernatant by centrifugation at $16,000 \times g$ for 1 min. Beads were then washed three times with 1m cold 1X PBS buffer. The bound protein was then denatured by addition of 30 μ l 2X protein sample buffer and boiling at 95 °C for 5 min. Ten microlitres of the sample was analyzed in Western blots with anti-Nus·Tag Ab as above.

2.6. Mammalian expression constructs of HIV-1 *pro-fs* and Trx

CFP-and YFP-tagged pro-fs constructs were made previously (Su and Taylor, unpublished data). To make CFP-and YFP-tagged Trx constructs, Trx-wt and Trx-CS coding region was amplified by PCR from Flag-tagged Trx constructs, which were provided by Dr. Wang Min [49], using sense primer Trx-EcoRI, 5-GGT GGA ATT CGC CTT GTG GTA-3, containing a *EcoRI* site, and anti-sense primer Trx-XbaI, 5-CGG GCC CTC TAG ACT TAG AC-3, containing a *XbaI* site. The PCR product was then digested by *EcoRI* and *XbaI* and cloned into *EcoRI* and *XbaI* sites in vectors pECFP-C1 and pEYFP-C1 (Clontech). The fusion constructs were CFP-or YFP-tagged at N-terminus of Trx-wt and Trx-CS (Fig. 4). All expression constructs were then transformed into *E. coli* strain DH5 α using chemical transformation method followed by extraction and purification using QIAprep Miniprep Kits (Qiagen). Fidelity of the construct was verified by automated DNA sequencing (Molecular Genetics Instrumentation Facilities, University of Georgia).

2.7. Mammalian cell culture and transient transfection

HEK 293 T cell culture was maintained in Dulbecco's modified Eagle's medium (DMEM) with 4 mM l-glutamine adjusted to contain 1.5 g/L sodium bicarbonate and 4.5 g/L glucose, 90% (Sigma), supplemented with 10% fetal bovine serum (FBS) at 37 °C with 5% CO₂. Cells were transiently transfected using lipofectamine 2000 (Invitrogen) following manufacture's instructions. For subcellular localization studies of Trx, cells were thinly plated on polylysine-coated 25 mm glass coverslips with 8×10^5 cells in 35 mm dish. For FRET experiments, cells were plated in six-well plate at 8×10^5 cells/well 24 h before transfection. Different amount of fluorescent constructs were used in transfection, ranging from 0.5 to 3.0 μ g for six-well plate. The purpose was to achieve a similar expression level across different CFP-and YFP-tagged constructs, judged by intensity of fluorescence detected by Luminescent Spectrometer LS55 (Perkin-Elmer) (Su and Taylor, unpublished data). Cells were treated with or without phorbol 12-myristate 13-acetate (PMA, 50 ng/ml, Sigma) 16 h post-transfection, and incubated for additional 24 h before subjecting to the subcellular localization study and confocal FRET microscopy.

2.8. Subcellular localization study of Trx

It was previously demonstrated that pro-fs localizes in the nuclei of mammalian cells (Su and Taylor, unpublished data). The same method was applied to determine the subcellular localization of Trx-wt and Trx-CS. Briefly, a Zeiss fluorescent microscope equipped with green fluorescent and UV filters were used, allowing the visualization of green (YFP) and blue fluorescence (4,6-diamidino-2-phenylindole (DAPI) nuclear staining) of the YFP-Trx-wt in the transfected cells. DAPI nuclear staining permits the distinction between cytoplasmic and nuclear distributions. Cells were selected for imaging if stained with DAPI and successfully expressing YFP-Trx-wt. Two consecutive images were taken for each selected region of cells: with UV filter and with green fluorescent filter. Images were then overlaid digitally (Photoshop 7.0) to observe the subcellular localization of fluorescence-tagged Trx.

2.9. FRET data acquisition using confocal microscopy and analysis

FRET experiments were carried out as follows. Briefly, acceptor photobleaching method [54], [55] was used to assess FRET efficiency in transfected 293 T cells using confocal microscopy. The fluorescent detection channels were set to 465–485 nm (for CFP) and 520–565 nm (for YFP) on a Leica SP2 confocal microscope (Leica Microsystems, Germany). FRET efficiency was calculated according to the formula:

$$\text{FRET}_{\text{Eff}} = \frac{(D_{\text{post}} - D_{\text{pre}})}{D_{\text{post}} \text{ for all } D_{\text{post}} > D_{\text{pre}}}$$

where D_{pre} represents the emitted donor fluorescence before and D_{post} , after photobleaching of the acceptor [55]. To limit the effect of heterogeneity of expression levels, only cells with similar expression level of CFP-tagged and YFP-tagged constructs across different transfections were selected. The individual cell nuclei were selected as area of interests (ROIs). Two independent transfections were performed, and 10–15 ROIs were selected for the measurement. FRET_{Eff} of all of the ROIs from all transfections were analyzed using ANOVA and Tukey's test (SAS Institute, Cary, NC) at $p = 0.05$.

Appropriate controls are needed to justify the possible “false-positive” detection of energy transfer since intensity-based FRET analysis is subject to direct fluorescent contribution from both CFP and YFP. A CFP-YFP concatemer was used as positive control, in which the CFP fluorophore and the YFP fluorophore were joined together with a short linker of nine amino acid residues (a generous gift from Dr. R.I. Morimoto's lab, Northwestern University, Chicago, IL). Strong energy transfer was expected to occur between the two fluorophores when this construct was expressed in cells. FRET signal were recorded for seven different transfections for studying interaction between Trx-wt and pro-fs: (1) negative control 1: CFP-Trx-wt alone; (2) negative control 2: YFP-pro-fs alone; (3) negative control 3: CFP-Trx-wt and YFP vector; (4) negative control 4: YFP-pro-fs and CFP vector; (5) CFP-Trx-wt and YFP-pro-fs, not treated with PMA; (6) CFP-Trx-wt and YFP-pro-fs, treated with PMA; (7) positive control: CFP-YFP concatemer. FRET was also carried out to determine interaction between YFP-Trx-wt and CFP-pro-fs, CFP-Trx-CS and YFP-pro-fs as described above.

3. Results

3.1. Bacterial expression and purification of Nus-*pro-fs* and Nus proteins

For all of the experiments described, we used the double Cys mutant (i.e., Sec to Cys) of pro-fs, which was necessary both to express and purify the protein in bacteria, and to achieve near-stoichiometric expression levels of fluorescent protein conjugates (with and without pro-fs attached) in mammalian cells. In the remainder of this paper, we will refer to this double Cys mutant of pro-fs simply as pro-fs. As described in Section 2, various fusion protein constructs were generated, in order to label pro-fs for the appropriate experiments. For co-immunoprecipitation and GST-pull down assays, pro-fs was fused to the Nus-Tag, for which a commercial Ab is available; a construct expressing Nus alone was used as a control in these experiments.

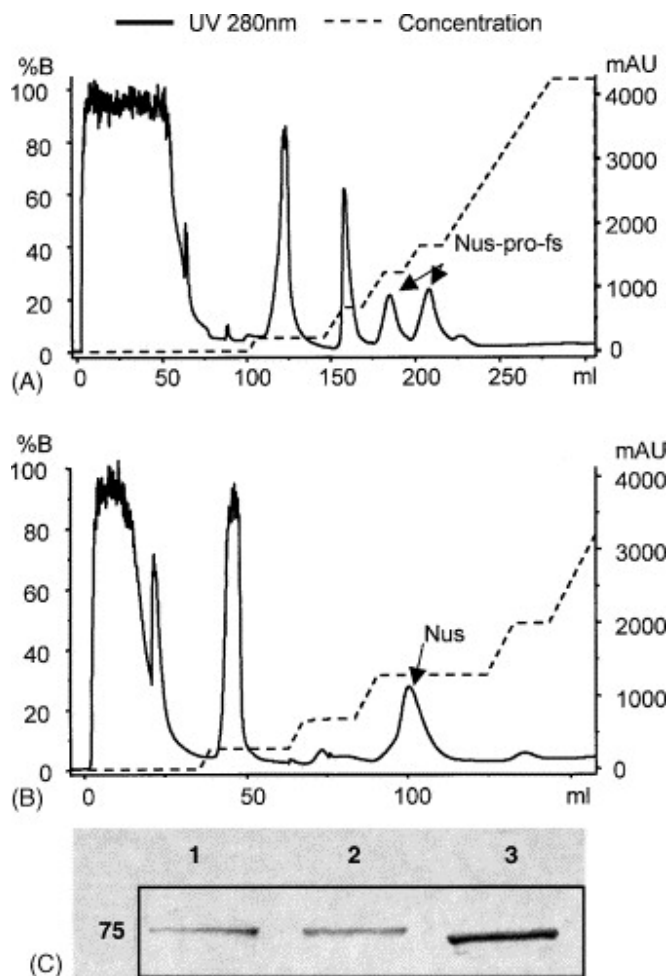


Fig. 2. HPLC chromatographs of the purification of Nus-*pro-fs* and Nus proteins expressed in *E. coli* BL21 (DE3) and Western blot analysis. The solid line represents the reading of UV₂₈₀ and the dashed line represents the concentration of buffer B. (A) Column separation of whole cell lysate of bacteria expressing Nus-*pro-fs*. There are two peaks containing Nus-*pro-fs* as shown on the HPLC chromatograph when the proportion of buffer B reached 16.1 and 23.9%. (B) Column separation of whole cell lysate for bacteria expressing Nus protein. Nus protein was eluted from the column when buffer B reached 31%. (C) Western blot of Nus-*pro-fs* and Nus proteins using Nus-Tag antibody (Novagen). Lane C1 shows the first HPLC peak of Nus-*pro-fs* protein, lane C2 shows the second HPLC peak of Nus-*pro-fs*, lane C3 shows the HPLC peak of Nus protein.

The time courses of expression of Nus-pro-fs and Nus in *E. coli* were analyzed in 10% Tris-HCl SDS-PAGE gel (data not shown). Both Nus-pro-fs and Nus proteins were detected in the supernatants of sonicated bacteria when induced by IPTG at 30 °C, which indicates that the proteins are folded into their native form. Nus-pro-fs has Nus·Tag at the N-terminus and pro-fs at the C-terminus with a molecular mass of 75 kDa, whereas Nus protein lacks the pro-fs domain and has a molecular mass of approximately 65 kDa (Fig. 1).

There was one peak fraction from HPLC purification containing Nus protein as shown by Western blot analysis using Nus·Tag Ab (Fig. 2, panel C). This peak eluted when buffer B reached 31% (Fig. 2, panel B). In contrast, there were two successive peaks from HPLC purification (Fig. 2, panel A) containing Nus-pro-fs protein, as shown by Western blot analysis using Nus Tag Ab (Fig. 2, panel C). One of the two peaks eluted on the HPLC chromatograph when the proportion of buffer B reached 16.1%, the other eluted when buffer B reached 23.9% (Fig. 2, panel A). The first fraction of Nus-pro-fs had about 70% homogeneity and the second had more than 90% homogeneity as assessed by SDS-PAGE (data not shown). The high purity of the protein allowed us to examine the interaction between pro-fs and Trx in vitro.

3.2. Co-immunoprecipitation of pro-fs and Trx and GST-pull down assay demonstrate a specific interaction between the two proteins

Based upon the sequence similarity between pro-fs and the DNA binding loop of NF- κ B, we hypothesize that pro-fs interacts with Trx. To assess this interaction in vitro, fusion protein Nus-pro-fs was co-immunoprecipitated with human Trx protein using anti-Trx Ab via incubation with Protein A magnetic beads. Western blots of the elution products showed that Nus-pro-fs was not detected from incubation with beads and anti-Trx in the absence of Trx (Fig. 3A, lane 1), and no Nus protein band was detected from incubation with Trx and anti-Trx (Fig. 3A, lane 2). Only the combined Trx + Nus-pro-fs gave a strong positive band (Fig. 3A, lane 3), showing that Nus-pro-fs bound to the beads and anti-Trx only in the presence of Trx, and that the pro-fs domain was required for that binding.

We then examined whether the two Cys residues in the active center of Trx are essential for the interaction between Trx and pro-fs, by comparing interactions between Trx-wt + pro-fs and Trx-CS + pro-fs. Two GST-Trx fusion proteins were used for this experiment. When Nus-pro-fs was incubated with GSH beads alone, Nus-pro-fs was not detected on the Western blot (Fig. 3B, lane 1), indicating that there is no non-specific binding of Nus-pro-fs to the GSH beads. Nus-pro-fs was detected in a Western blot with anti-NusTag Ab from incubation with either GST-Trx-wt or GST-Trx-CS (Fig. 3B, lane 2 and 3). A stronger signal of Nus-pro-fs was shown when the protein was incubated with GST-Trx-wt than with GST-Trx-CS. The control protein Nus was not detected in the Western blot from incubation with either GST-Trx-wt or GST-Trx-CS fusion proteins (Fig. 3B, lane 4 and 5). Therefore, the two Cys residues in the redox center of Trx are not essential for its binding to pro-fs.

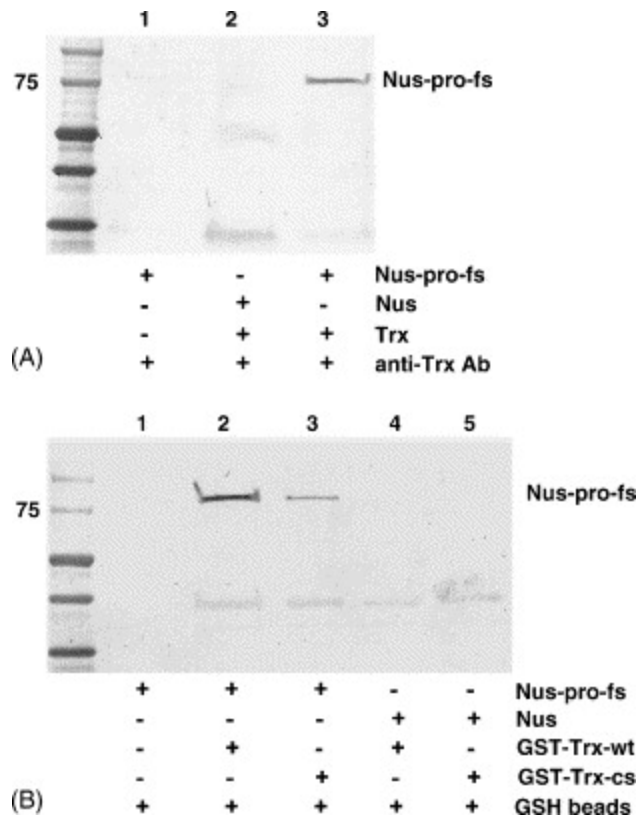


Fig. 3. Co-immunoprecipitation of Nus-pro-fs and human thioredoxin (Trx), and GST-pull down assay of pro-fs. (A) Nus-pro-fs and rabbit polyclonal anti-Trx Ab were mixed without (lane 1) or with (lane 3) human Trx protein and incubated overnight at 4 °C. The mixture was then added to protein A magnetic beads to incubate for 1 h at 4 °C. Nus protein was used to incubate with Trx and Trx Ab by the same procedure, as a negative control (lane 2). After washing, eluting and Western blotting with mouse anti-Nus monoclonal Ab, only combined Trx + Nus-pro-fs gave a strong positive band (lane 3). (B) Nus-pro-fs were added to glutathione-Sepharose beads alone (lane 1) or beads bound with wild-type GST-Trx fusion protein (GST-Trx-wt, lane 2) or a mutant GST-Trx fusion protein (GST-Trx-CS, lane 3), in which Trx residues Cys32 and Cys35 were mutated to Ser. Nus protein was added to GST-Trx-wt (lane 4) or GST-Trx-CS (lane 5) as negative controls. After incubation, the bound protein was denatured and subjected to Western blotting with anti-Nus-Tag Ab as above. Nus-pro-fs but not Nus alone was detected in the Western blot. The stronger band in lane 2 as compared to lane 3 suggests that pro-fs binds Trx-wt with higher affinity than to Trx-CS.

3.3. Expression and subcellular localization of Trx in mammalian cells

Each one of the eight constructs (Fig. 4) was successfully expressed in 293 T, MDCK and HeLa cells and could be visualized in living cells using fluorescent or confocal microscopy. Previously, we found that pro-fs localizes in cell nuclei in these cell lines (Su and Taylor, unpublished data). It was reported that Trx predominantly localizes in the cytoplasm, and treatments with UV irradiation, PMA (50 ng/ml) or TNF- α (100 ng/ml) induce the translocation of Trx into the nucleus [48]. We then examined whether PMA treatment alters the subcellular localization of fluorescent-tagged Trx fusion protein, YFP-Trx-wt or YFP-Trx-CS. In transfected cells not treated with PMA, YFP-Trx-wt was visualized in both cytoplasm and the nuclei in 293T cells (Fig. 5A, left panel), the latter of which was confirmed with DNA counterstain with DAPI nuclear staining (Fig. 5B, left panel), but with the majority of found protein in the cytoplasm.

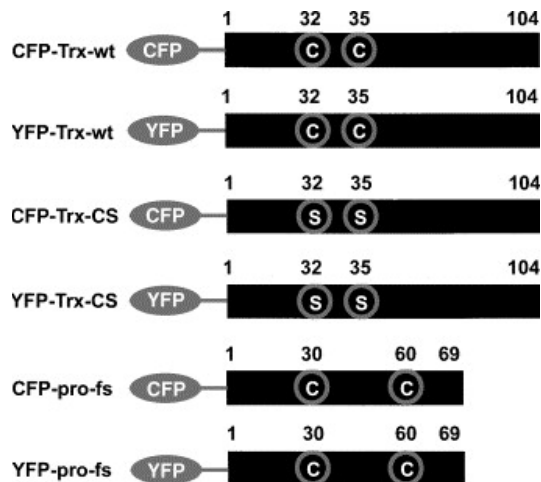


Fig. 4. Schematic structures of N-terminal CFP- or YFP- tagged Trx-wt, Trx-CS and *pro-fs* constructs. Artificial linkers constructed from the polylinker region of pECFP-C1 and pEYFP-C1 (Clontech) are drawn in gray lines. All fusion constructs were CFP- or YFP-tagged at their N-termini. Trx-CS is a double mutant generated from Trx-wt, with two Ser residues in place of Cys residues in the active center [49]. In order to express *pro-fs* in sufficient amount for FRET studies, we continued to use the mutant *of pro-fs*, with two Cys residues in the place of potential Sec residues, which are encoded by UGA codons in the wild-type *pro-fs*.

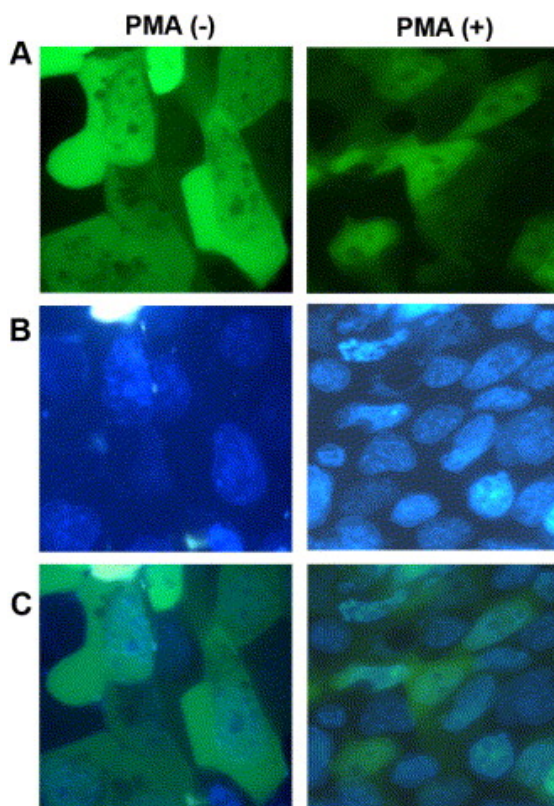


Fig. 5. Effect of PMA treatment on subcellular localization of YFP-Trx-wt in 293 T cells. Cells were transiently transfected with YFP-Trx-wt and were treated with (right panel) or without (left panel) PMA (50 ng/ml) 16 h post-transfection. After another 24 h incubation, cells were stained with DAPI nuclear staining (blue fluorescence) and visualized with UV filter (A) or green fluorescent filter (B). A merged image of the two panels is shown in (C), which verifies subcellular localization of YFP-Trx-wt. In cells untreated with PMA, YFP-Trx-wt predominantly localizes in the cytoplasm then in the nuclei (A, left panel), whereas in PMA-stimulated cells, more YFP-Trx-wt localizes in the cell nuclei than in the cytoplasm (A, right panel).

The merged image verifies this subcellular localization of YFP-Trx-wt (Fig. 5C, left panel). Treatment with PMA led to an enhanced fluorescent intensity in the nuclei with a decrease in the cytoplasm of 293 T cells, indicating that PMA treatment was associated with the nuclear translocation of YFP-Trx-wt (Fig. 5A–C, right panel). Similar results were observed in YFP-Trx-CS transfected cells (data not shown).

3.4. Trx interacts with pro-fs in PMA-stimulated 293 T cells

We employed confocal FRET microscopy to study the protein–protein interaction between Trx and pro-fs in living cells. In the FRET assay, fairly high (and approximately equal) expression levels of *both* of the fluorescent-tagged proteins are required in order to correctly detect the energy transfer. The inefficiency and complexity of selenoprotein production in mammalian cells would result in a very low level of fluorescence-tagged wild-type pro-fs expression, so that it would probably be impossible to detect any FRET signal. Hence, we continued to use the double Cys mutant of pro-fs in our confocal FRET microscopy studies, particular since we had already established that the Cys mutant of pro-fs binds Trx with high affinity in cell-free systems. The acceptor photobleaching method was used to measure both the quenching of the donor signal and the sensitized acceptor emission to confirm the occurrence of FRET, and to eliminate the effect caused by different expression levels of the constructs within cells and inhomogeneities in the thickness of the cells. YFP-pro-fs and CFP-Trx-wt or CFP-Trx-CS were transiently co-transfected into 293 T cells. Fig. 6 demonstrates representative images observed from the CFP and YFP channels during acceptor photobleaching, and the resulting FRET images derived using the formula described in Section 2. Numerical values from each channel represent the intensity of the signal, but do not encode color information. All colors are artificially assigned. Signals from the YFP channel are presented as yellow, signals from CFP channel as cyan, and signals for FRET are shown in pseudocolor. The color images in Fig. 6 do illustrate the distribution of CFP-pro-fs and YFP-Trx-wt.

The acceptor photobleaching method was used to measure both the quenching of the donor signal and the sensitized acceptor emission to confirm the occurrence of FRET, and to eliminate the effect caused by different expression levels of the constructs within cells and inhomogeneities in the thickness of the cells. YFP-pro-fs and CFP-Trx-wt or CFP-Trx-CS were transiently co-transfected into 293 T cells. Fig. 6 demonstrates representative images observed from the CFP and YFP channels during acceptor photobleaching, and the resulting FRET images derived using the formula described in Section 2. Numerical values from each channel represent the intensity of the signal, but do not encode color information. All colors are artificially assigned. Signals from the YFP channel are presented as yellow, signals from CFP channel as cyan, and signals for FRET are shown in pseudocolor. The color images in Fig. 6 do illustrate the distribution of CFP-pro-fs and YFP-Trx-wt.

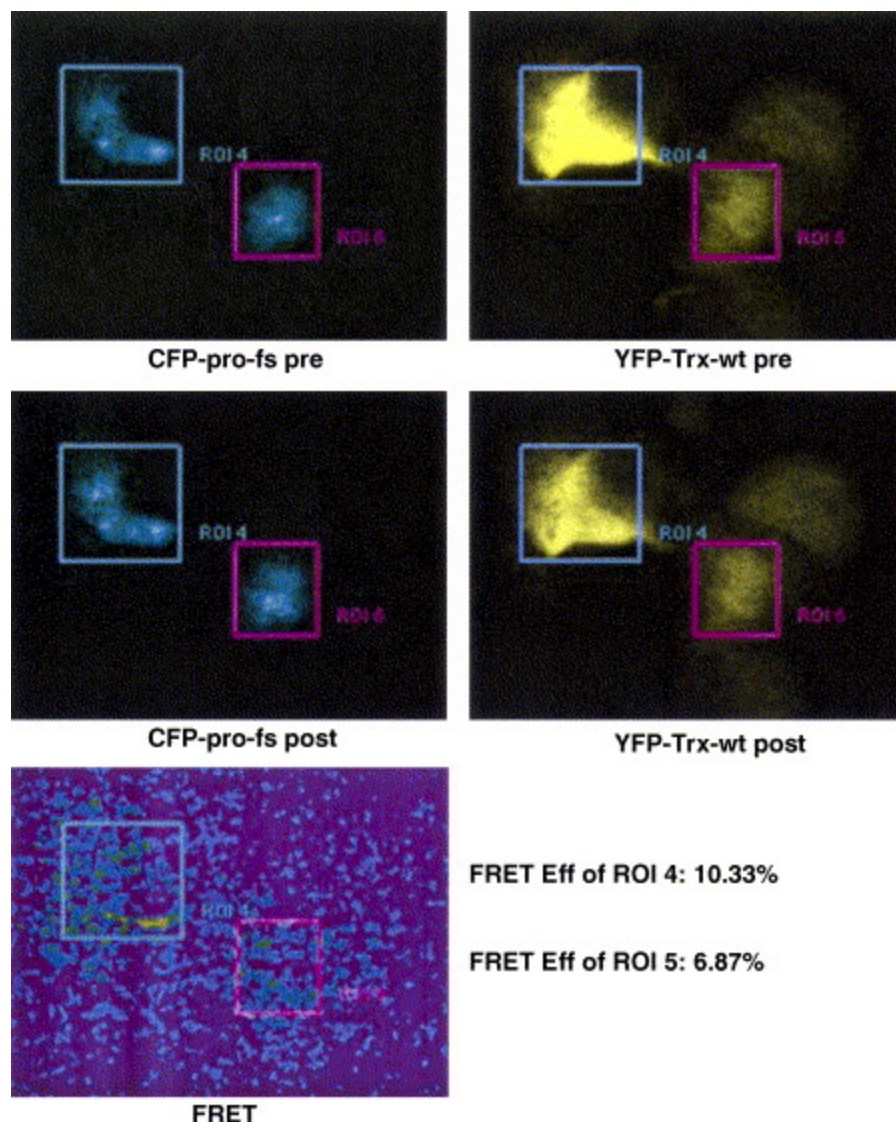


Fig. 6. Representative FRET images by confocal microscopy through photobleaching process. 293 T cells were transfected with CFP-pro-fs and YFP-Trx-wt. Transfected cells were stimulated with PMA (50 ng/ml) 16 h post-transfection. FRET signal acquisition was carried out after another 24 h incubation via acceptor photobleaching method using confocal microscope. Cells were only analyzed when both tagged proteins were expressed at similar level. Images represent fluorescent signals observed from two channels through photobleaching process. Individual nucleus was selected as area of interest and FRET image was obtained as described in Section 2. *Pre* stands for before photobleaching and *post* after photobleaching. All colors are arbitrarily assigned to indicate signal strength. FRET efficiency is represented as pseudocolor.

A CFP-YFP concatemer, in which CFP and YFP are covalently linked, was used as a positive control for these studies. Using the equation described in Section 2, expression of the CFP-YFP concatemer produced a FRET signal of 27% (Fig. 7). Since the generation of FRET requires the presence of both CFP and YFP fluorophores, single transfection of one fluorophore should not produce any FRET signal. Based on the theory behind the FRET method, co-expression of unlinked YFP and CFP fluorophores should not generate FRET signal unless they are in direct contact. With the negative controls employed in this experiment, there were only marginal FRET signals detected (less than 1%) (Fig. 7). These include cells singly transfected with only CFP-or YFP-tagged Trx-wt, Trx-CS or pro-fs, co-transfected with CFP-pro-fs and the YFP vector pair,

YFP-pro-fs and the CFP vector pair, CFP-Trx-wt or -CS and YFP vector pair, YFP-Trx-wt or-CS and the CFP vector pair. Thus, there was no energy transfer between these proteins. FRET efficiency in the positive control was significantly higher than that in all the negative controls ($p < 0.0001$).

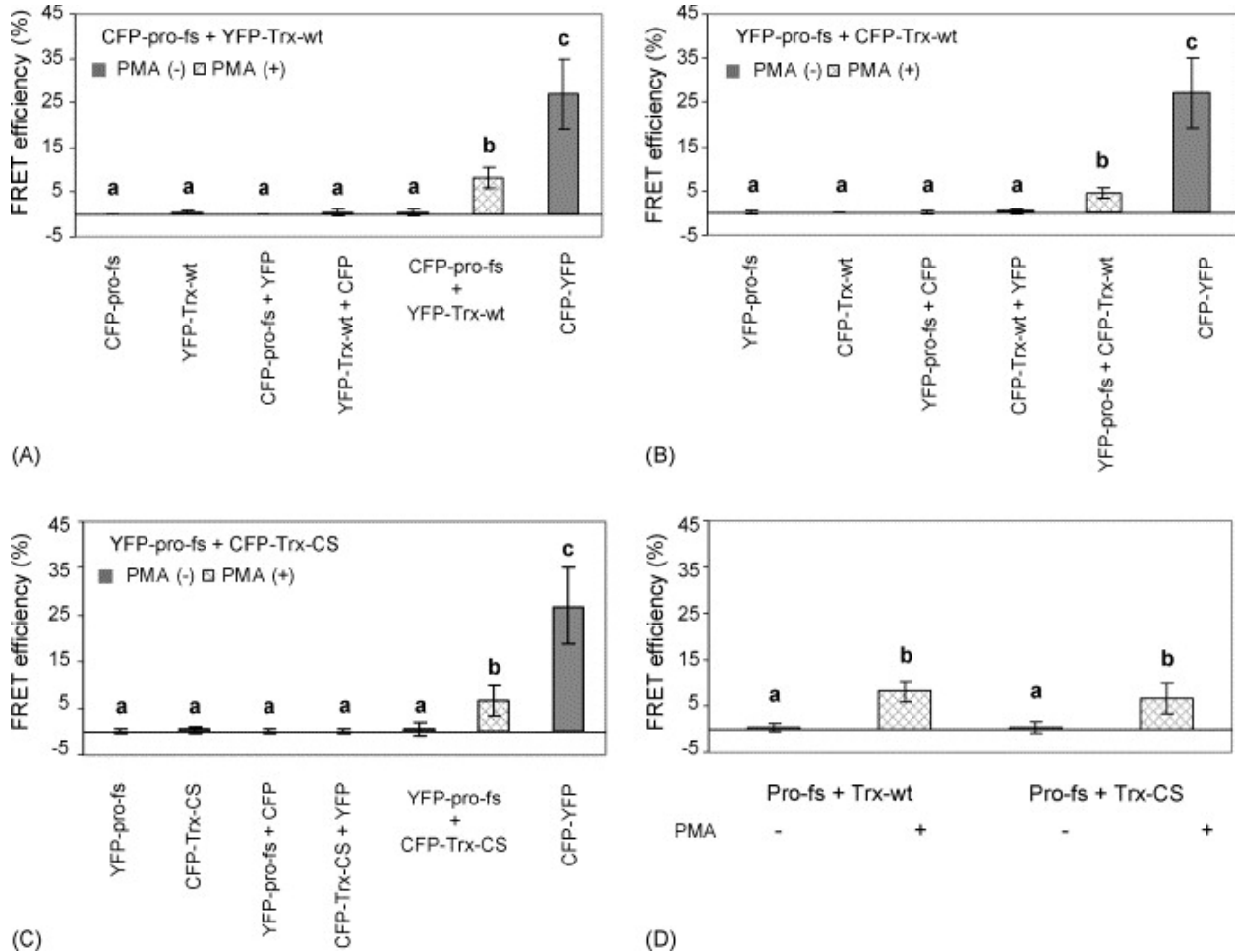


Fig. 7. Interaction between thioredoxin (Trx) and pro-fs detected in PMA-stimulated cells by FRET using confocal microscopy. HEK 293 T cells were transfected with different expression constructs as shown in the graphs. CFP-YFP is a construct that CFP and YFP fluorophores are directly linked. FRET_{Eff} of all samples were analyzed using ANOVA and Tukey's test (SAS Institute, Cary, NC) at $P = 0.05$. In all of the graphs, the solid gray bars represent cells not treated with PMA, whereas the white bars with gridlines represent cells treated with PMA. (A) FRET efficiency in PMA-stimulated cells co-expressing CFP-pro-fs and YFP-Trx-wt is significantly higher than that in unstimulated cells co-expressing both proteins and all negative controls, but is significantly lower than that in CFP-YFP transfected cells. (B) Significant FRET efficiency was also detected in PMA-stimulated cells co-expressing YFP-pro-fs and CFP-Trx-wt. (C) FRET efficiency detected in PMA-stimulated cells co-expressing YFP-pro-fs and CFP-Trx-CS is significantly higher than in unstimulated cells co-expressing both proteins and all of the negative controls, is significantly lower than in CFP-YFP transfected cells. (D) There is no significant difference between FRET efficiencies detected in PMA-stimulated cells co-expressing CFP-pro-fs + YFP-Trx-wt and YFP-pro-fs + CFP-Trx-CS, which are both significantly higher than that in unstimulated cells.

In PMA-stimulated cells co-expressing CFP-pro-fs and YFP-Trx-wt, YFP-pro-fs and CFP-Trx-wt, and YFP-pro-fs and CFP-Trx-CS, FRET efficiency was detected at 8.2, 4.6, and 6.6%, respectively (Fig. 7A–D), which are all significantly higher than all negative controls

($p < 0.0001$). However, FRET efficiency detected between pro-fs + Trx-wt and pro-fs + Trx-CS do not significantly differ from each other (Fig. 7D). In cells unstimulated with PMA, co-expression of CFP-pro-fs and YFP-Trx-wt, and YFP-pro-fs and CFP-Trx-CS gave only marginal FRET signals, 0.4 and 0.5%, respectively, and thus showed no significant difference from the negative controls (Fig. 7A and C). In summary, FRET efficiency between Trx and pro-fs in PMA-stimulated cells were intermediate between unstimulated and positive controls in mammalian cells.

4. Discussion

The results of our cell-free in vitro studies demonstrate that the putative HIV-1 encoded peptide, pro-fs, is a target of the cellular redox protein Trx (or vice-versa). Both co-immunoprecipitation and GST-pull down results consistently showed that pro-fs binds to human Trx in vitro (Fig. 3); moreover, the binding affinity is apparently stronger with Trx-wt than with Trx-CS, in which the two Cys residues in the active center of Trx are mutated to Ser (Fig. 3B). These results strongly suggest that the mutation of the 2 pro-fs UGA codons to Cys codons do not substantially interfere with the structure and Trx-binding ability of pro-fs.

Consistent with previous studies in HeLa cells, where PMA was shown to efficiently induce translocation of Trx into the nucleus [56], we observed the nuclear translocation of fluorescence-tagged Trx in response to PMA stimulation (Fig. 5). Then, using FRET, we demonstrated that pro-fs interacts with Trx in PMA-stimulated cells (Fig. 6, Fig. 7), which is consistent with the results of our in vitro studies (Fig. 3). Both wild type (Trx-wt) and the double Cys mutant (Trx-CS) of Trx bind to pro-fs in PMA-stimulated cells; however, the FRET was barely detectable in cells untreated with PMA (Fig. 7), suggesting that the Trx-pro-fs interaction occurs predominantly in the cell nuclei. This was not unexpected, because we have previously observed that pro-fs localizes exclusively in the cell nucleus in 293 T, MDCK and HeLa cells (Su and Taylor, unpublished data).

The fact that pro-fs interacts not only with Trx-wt but also with the mutant Trx-CS (which lacks the Trx active site Cys residues) rules out the possibility that the interaction between pro-fs and Trx could simply be due to cross-linkage via non-specific formation of an intermolecular disulfide bond between the Cys residues of pro-fs and the Cys residues in the active site of Trx. Rather, these findings suggest that Trx-pro-fs binding is a structurally specific interaction that involves multiple amino acid residues in the interactive region. This observation is consistent with molecular modeling results (Taylor et al., unpublished data) which predicts that at least eight amino acid residues of pro-fs are involved in the protein-protein interaction, and that, based on calculated non-bonded energy terms, Trx binds to the “active site” peptide of pro-fs at least as favorably as it binds to its known substrate, the DNA binding loop of NF- κ B.

Taken as a whole, our results unequivocally demonstrate a high affinity molecular interaction between Trx and the HIV-1 encoded transframe peptide which we call pro-fs, at least when the UGA codons of wild type pro-fs are mutated to Cys codons. This begs the question: what is the functional significance of this interaction in terms of potential mimicry of NF- κ B by pro-fs? To answer that question, the following facts must be considered: (1) Trx is a redox protein involved in dithiol/disulfide exchange; (2) in most of its interactions with target proteins, Trx acts as a

reducing agent, with the exception that; (3) oxidized Trx is reduced by TR, which is a selenoprotein in mammals [57] and *C. elegans* [57]. Particularly because, like TR, wild type pro-fs is a putative selenoprotein, it is therefore important to consider both the possibilities, i.e., that (1) like NF- κ B, pro-fs may be a target for reduction by Trx, or alternatively, that (2) pro-fs may act as a virally-encoded TR, that serves to maintain Trx in a reduced state, particularly in the cell nucleus. These two alternatives will be discussed in more detail in the following paragraphs.

Regarding redox regulation of NF- κ B by Trx, although reduced Trx *inhibits* NF- κ B activation in the cytoplasm, upon nuclear translocation of NF- κ B and Trx, reduced Trx *enables* the DNA binding activity of NF- κ B [48], by reducing the Cys residue in the DNA/Trx recognition loop—the Cys that aligns with the first UGA codon of pro-fs [7]. Thus, it is possible that pro-fs may simply be another substrate that must be reduced by Trx in order to mediate its effects, which could include direct mimicry of the DNA-binding ability of NF- κ B, as discussed previously [7]. Consistent with that possibility, using a HIV-1 LTR-*lacZ* reporter system, we have found that pro-fs is a potent activator of HIV-1 LTR and functions via NF- κ B recognition sites in the LTR (Taylor et al., unpublished data), suggesting that pro-fs may function as a mimic of NF- κ B in activation not only of HIV-1 transcription, but also of hundreds of cellular genes regulated by NF- κ B that are involved in host immune responses, such as cytokines, adhesion molecules and genes regulating apoptosis. HIV could directly manipulate host cellular defenses by this mechanism.

However, the very small size of pro-fs relative to NF- κ B tends to favor the alternative hypothesis: that perhaps its mode of action is simply to chemically *reduce* Trx, in order for Trx to activate NF- κ B in the nucleus, which would indirectly stimulate the viral LTR as we have observed. As opposed to the previously discussed possibility that Trx may serve as a reducing agent to pro-fs, the direct and structurally specific interaction between Trx and pro-fs may enable pro-fs to act as a nuclear TR-like molecule to store up and deliver the necessary reducing equivalents to Trx in the midst of oxidizing intracellular environments, thereby enhancing NF- κ B activation in the nucleus to promote HIV-1 replication.

The structurally specific association between pro-fs and Trx also suggests that pro-fs might participate in other functions of Trx. It was shown that Trx plays a key role in inhibiting apoptosis of HIV-infected cells while simultaneously inducing apoptosis of bystander cells via upregulation of FasL. This mechanism requires the direct association of Trx with the N-terminal portion of apoptosis signaling kinase 1 (ASK1), a key component of TNF- α -induced apoptosis [58]. There is evidence indicating that HIV-1 *nef* protein participates in this process by preventing disassociation of Trx and ASK1 in HIV infected cells [59]. Thus, based on the interaction between Trx and pro-fs, it is possible that HIV-1 encoded pro-fs might also participate in the regulation of apoptotic processes via Trx in infected and bystander cells. Another important role of Trx is that it acts as a hydrogen donor for ribonucleotide reductase, which is essential for DNA synthesis [57]; thus, Trx is required by retroviruses for formation of their proviral DNA. By associating with and possibly reducing Trx, pro-fs might contribute to viral DNA synthesis. Trx is also known to regulate the DNA binding ability of another redox-responsive transcription factor, activator protein-1 (AP-1), which also regulates HIV transcription by binding to HIV LTR [60], [61]. Therefore, by directly interacting with Trx, pro-fs could possibly play a role in the redox regulation of AP-1 activated HIV-1 replication.

The role of ROS and oxidative stress in HIV pathogenesis has received considerable attention in recent years, due to their roles in inducing activation of HIV transcription. NF- κ B was the first transcription factor found to respond to oxidative stress mediated by prooxidants and pathogenic stimuli [23], [24], [25], [26]. Conversely, this activation can be inhibited by antioxidants, including Se, glutathione, NAC, and the cellular selenoprotein GPx [28], [29], [30]. It has been reported that low dose Se supplementation can suppress NF- κ B activation in response to TNF- α and H₂O₂ in vitro, via increased production of GPx [31]. Hence, it seems reasonable that viruses might encode selenoproteins to directly intervene in host redox regulation pathways, e.g., to protect themselves against cellular ROS-mediated defensive mechanisms such as apoptosis. Via selenoprotein synthesis, a virus could hijack the Se in host cells and cause a decline of cellular selenoprotein production [62]. *Molluscum contagiosum*, a poxvirus that causes persistent skin neoplasms in children and acquired immunodeficiency syndrome (AIDS) patients, encodes a functional GPx enzyme [63], [64]. It was shown to protect human keratinocytes against cytotoxic effects of ultraviolet irradiation and hydrogen peroxide, which provides a mechanism for a virus to defend itself against environmental stress [64]. HIV-1 has been shown to encode a highly truncated GPx enzyme that showed measurable GPx activity and protects cells from oxidant-induced apoptosis [1], [65], [66]. Thus, it is not unprecedented that HIV-1 might encode a selenoprotein to optimize its replication and survival in an oxidation-prone environment.

It must be pointed out that pro-fs is still a hypothetical protein, predicted based on a bioinformatic analysis of the HIV-1 genome. There are several possibilities why pro-fs has escaped detection in infected patients. Pro-fs can only be expressed as a double frameshift protein, since it is encoded in the overlapping -1 reading frame of the HIV-1 protease coding region, which, as part of the *pol* gene, is also encoded via a -1 frameshift from the *gag* coding region. Due to the inefficiency of ribosomal frameshifting, which only occurs in about 1–10% of translational events [1], pro-fs only has 1% or less opportunity to be expressed as compared to HIV structural proteins—probably much less, when the inefficiency of decoding UGA as Sec is also considered. This would result in a very low abundance of pro-fs in HIV-infected cells. Another factor might be the very low molecular mass of pro-fs, approximately either 7.2 or 8.3 kDa, depending on whether one or both in-frame UGA codons are decoded as Sec. However, it is noteworthy that in a study of the effect of HIV-1 infection on selenoprotein expression in ⁷⁵Se-labeled human Jurkat T cells, low molecular mass Se-labeled compounds in HIV-infected cells were detected (Fig. 1B in [67]). The position of a wide band partially overlapping a known 6 kDa cellular selenoprotein is in the correct size range to correspond to predicted isoforms of pro-fs.

In this study, we have shown that an HIV-1 encoded peptide, pro-fs, mimics the ability of NF- κ B to bind to human Trx with high affinity, both in vitro and in living cells; this interaction is structurally specific. We have also demonstrated that upon stimulation by PMA, human Trx translocates into the nucleus from the cytoplasm, and that pro-fs interacts with Trx in the cell nuclei. Given the complexity of the multiple factors involved, consideration of the outcome of this interaction in host cellular response in regard to HIV-1 infection and disease progression merits further exploration.

Acknowledgments

We would like to thank Dr. Robert J. Hondal (University of Vermont, Burlington, VT) for providing us the original expression construct for pro-fs, and Dr. Richard I. Morimoto (Northwestern University, Chicago, IL) for providing the CFP-YFP construct. This work was supported by PHS Grant DA13561 (E.W.T., PI) from the National Institute on Drug Abuse (NIDA).

References

- [1] E.W. Taylor, C.S. Ramanathan, R.K. Jalluri, R.G. Nadimpalli, Abasis for new approaches to the chemotherapy of AIDS: novel genes in HIV-1 potentially encode selenoproteins expressed by ribosomal frameshifting and termination suppression, *J. Med. Chem.* 37 (1994) 2637–2654.
- [2] E.W. Taylor, R.G. Nadimpalli, C.S. Ramanathan, Genomic structures of viral agents in relation to the biosynthesis of selenoproteins, *Biol. Trace. Elem. Res.* 56 (1997) 63–91.
- [3] M.J. Berry, L. Banu, J.W. Harney, P.R. Larsen, Functional characterization of the eukaryotic SECIS elements which direct selenocysteine insertion at UGA codons, *EMBO J.* 12 (1993) 3315–3322.
- [4] A. Bock, K. Forchhammer, J. Heider, W. Leinfelder, G. Sawers, B. Veprek, F. Zinoni, Selenocysteine: the 21st amino acid, *Mol. Microbiol.* 5 (1991) 515–520.
- [5] Q. Shen, F.F. Chu, P.E. Newburger, Sequences in the 3'-untranslated region of the human cellular glutathione peroxidase gene are necessary and sufficient for selenocysteine incorporation at the UGA codon, *J. Biol. Chem.* 268 (1993) 11463–11469.
- [6] E.W. Taylor, A.A. Bhat, R.G. Nadimpalli, W. Zhang, J. Kececioglu, HIV-1 encodes a sequence overlapping env gp41 with highly significant similarity to selenium-dependent glutathione peroxidases, *J. Acquir. Immune. Defic. Syndr. Hum. Retrovirol.* 15 (1997) 393–394.
- [7] E.W. Taylor, A.G. Cox, L. Zhao, J.A. Ruzicka, A.A. Bhat, W. Zhang, R.G. Nadimpalli, R.G. Dean Nutrition, HIV, and drug abuse: the molecular basis of a unique role for selenium, *J. Acquir. Immune. Defic. Syndr.* 25 (Suppl. 1) (2000) S53–S61.
- [8] E.W. Taylor, C.S. Ramanathan, R.G. Nadimpalli, A general method for predicting potential new genes in nucleic acid sequences: application to the human immunodeficiency virus, in: M. Witten (Ed.), *Computational Medicine, Public Health and Biotechnology*, World Scientific, 1996, pp. 285–309.
- [9] J. Qin, G.M. Clore, W.M. Kennedy, J.R. Huth, A.M. Gronenborn, Solution structure of human thioredoxin in a mixed disulfide intermediate complex with its target peptide from the transcription factor NF- κ B, *Structure* 3 (1995) 289–297.
- [10] B.A. Antoni, S.B. Stein, A.B. Rabson, Regulation of human immunodeficiency virus infection: implications for pathogenesis, *Adv. Virus Res.* 43 (1994) 53–145.
- [11] P. Baeuerle, D. Baltimore, A 65-kappaD subunit of active NFkappaB is required for inhibition of NF-kappaB by I kappaB, *Genes Dev.* 3 (1989) 1689–1698.
- [12] D.P. Bednarik, T.M. Folks, Mechanisms of HIV-1 latency, *AIDS* 6 (1992) 3–16.

- [13] S. Doerre, P. Sista, S. Sun, D. Ballard, W. Greene, The c-rel protooncogene product represses NF- κ B p65-mediated transcriptional activation of the long terminal repeat of Type 1 human immunodeficiency virus, *PNAS* 90 (1993) 1023–1027.
- [14] K. Kawakami, C. Scheidereit, R.G. Roeder, Identification and purification of a human immunoglobulin-enhancer-binding protein (NF-kappa B) that activates transcription from a human immunodeficiency virus type 1 promoter in vitro, *PNAS* 85 (1988) 4700–4704.
- [15] A.B. Rabson, H.-C. Lin, NF- κ B and HIV: linking viral and immune activation, in: K.-T. Jeang (Ed.), *HIV-1: Molecular Biology and Pathogenesis—Viral Mechanisms*, Academic Press, 2000, pp. 161–207.
- [16] A.S. Baldwin, The NF- κ B and I κ B proteins: new discoveries and insights, *Annu. Rev. Immunol.* 14 (1996) 649–681.
- [17] P.A. Baeuerle, D. Baltimore, NF- κ B: ten years after, *Cell* 87 (1996) 13–20.
- [18] G. Biswas, H.K. Anandatheerthavarada, M. Zaidi, N.G. Avadhani, Mitochondria to nucleus stress signaling: a distinctive mechanism of NF κ B/Rel activation through calcineurin-mediated inactivation of I κ B β , *J. Cell Biol.* 161 (2003) 507–519.
- [19] U. Siebenlist, G. Fransozo, K. Brown, Structure, regulation and function of NF- κ B, *Annu. Rev. Cell Biol.* 10 (1994) 405–430.
- [20] I. Stancovski, D. Baltimore, NF- κ B activation: the I κ B kinase revealed, *Cell* 91 (1997) 299–302.
- [21] B. Tian, A.R. Brasier, Identification of a nuclear factor kappa B-dependent gene network, *Recent Prog. Horm. Res.* 58 (2003) 95–130.
- [22] G. Waris, A. Livolsi, V. Imbert, J. Peyron, A. Siddiqui, Hepatitis C virus NS5A and subgenomic replicons activate NF- κ B via tyrosine phosphorylation of I κ B α and its degradation by calpain protease, *J. Biol. Chem.* (2003) M303248200.
- [23] G.E. Griffin, K. Leung, T.M. Folks, S. Kunkel, G.J. Nabel, Activation of HIV gene expression during monocyte differentiation by induction of NF-kappa B, *Nature* 339 (1989) 70–73.
- [24] R. Schreck, P. Rieber, P.A. Baeuerle, Reactive oxygen intermediates as apparently widely used messengers in the activation of the NF-kappa B transcription factor and HIV-1, *EMBO J.* 10 (1991) 2247–2258.
- [25] R. Schreck, K. Albermann, P. Bauerle, Nuclear factor κ B: an oxidative stress-response transcription factor of eukaryotic cells, *Free Rad. Res. Comm.* 17 (1992) 221–237.
- [26] K. Schulze-Osthoff, R. Beyaert, V. Vandevoorde, G. Haegeman, W. Fiers, Depletion of the mitochondrial electron transport abrogates the cytotoxic and gene-inductive effects of TNF, *EMBO J.* 12 (1993) 3095–3104.
- [27] K. Mitomo, K. Nakayama, K. Fujimoto, X. Sun, S. Seki, K. Yamamoto, Two different cellular redox systems regulate the DNA-binding activity of the p50 subunit of NF-kappaB in vitro, *Gene* 145 (1994) 197–203.

- [28] A. Beg, T. Finco, P. Nantermet, A. Baldwin Jr., Tumor necrosis factor and interleukin-1 lead to phosphorylation and loss of I kappa B alpha: a mechanism for NF-kappa B activation, *Mol. Cell. Biol.* 13 (1993) 3301–3310.
- [29] T. Henkel, T. Machleidt, I. Alkalay, M. Kronke, Y. Ben-Neriah, P.A. Baeuerle, Rapid proteolysis of I kappa B-alpha is necessary for activation of transcription factor NF-kappa B, *Nature* 365 (1993) 182–185.
- [30] C. Kretz-Remy, P. Mehlen, M. Mirault, A. Arrigo, Inhibition of I kappa B-alpha phosphorylation and degradation and subsequent NF-kappa B activation by glutathione peroxidase overexpression, *J. Cell Biol.* 133 (1996) 1083–1093.
- [31] V. Makropoulos, T. Briining, K. Schulze-Osthoff, Selenium-mediated inhibition of transcription factor NF kappa B and HIV-1 LTR promoter activity, *Arch. Toxicol.* 70 (1996) 277–283.
- [32] Y.J. Suzuki, B.B. Aggarwal, L. Packer, Alpha-lipoic acid is a potent inhibitor of NF-kappa B activation in human T cells, *Biochem. Biophys. Res. Commun.* 189 (1992) 1709–1715.
- [33] J.-P. Yang, J.P. Merina, T. Nakanoa, T. Katoa, Y. Kitadeb, T. Okamoto, Inhibition of the DNA-binding activity of NF-kappa B by gold compounds in vitro, *FEBS Lett.* 361 (1995) 89–96.
- [34] R.A. Sunde, Selenium, in: B.L. O'Dell, R.A. Sunde (Eds.), *Handbook of Nutritionally Essential Minerals*, Marcel Dekker, New York, 1997, pp. 493–556.
- [35] C. Allavena, B. Dousset, T. May, F. Dubois, P. Canton, F. Belleville, Relationship of trace-element, immunological markers, and HIV infection progression, *Biol. Trace Elem. Res.* 47 (1995).
- [36] M.A. Beck, Q. Shi, V.C. Morris, O.A. Levander, Rapid genomic evolution of a non-virulent coxsackievirus B3 in selenium-deficient mice results in selection of identical virulent isolates, *Nat. Med.* 1 (1995) 433–436.
- [37] M.K. Baum, G. Shor-posner, S. Lai, G. Zhang, H. Lai, M.A. Fletcher, H. Sauberlich, J.B. Page, High risk of HIV-related mortality is associated with selenium deficiency, *J. Acquir. Immune. Defic. Syndr. Hum. Retrovirol.* 15 (1997) 370–376.
- [38] J. Constans, J.L. Pellegrin, C. Sergeant, M. Simonoff, I. Pellegrin, H. Fleury, B. Leng, C. Conri, Serum selenium predicts outcome in HIV infection, *J. Acquir. Immune. Defic. Syndr. Hum. Retrovirol.* 10 (1995) 392.
- [39] B.M. Dworkin, Selenium deficiency in HIV infection and the acquired immunodeficiency syndrome (AIDS), *Chem. Biol. Interact.* 91 (1994) 181–186.
- [40] S.Y. Yu, Y.J. Zhu, W.G. Li, Protective role of selenium against hepatitis B virus and primary liver cancer in Qidong, *Biol. Trace Elem. Res.* 56 (1997) 117–124.
- [41] M.W. Yu, I.S. Horng, K.H. Hsu, Y.C. Chiang, Y.F. Liaw, C.J. Chen, Plasma selenium levels and risk of hepatocellular carcinoma among men with chronic hepatitis virus infection, *Am. J. Epidemiol.* 150 (1999) 367–374.

- [42] K. Hori, D. Hatfield, F. Maldarelli, B.J. Lee, K.A. Clouse, Selenium supplementation suppresses tumor necrosis factor alpha-induced human immunodeficiency virus type 1 replication in vitro, *AIDS Res. Hum. Retroviruses* 13 (1997) 1325–1332.
- [43] R. Brigelius-Flohe, B. Friedrichs, S. Maurer, M. Schultz, R. Streicher, Interleukin-1-induced nuclear factor kappa B activation is inhibited by overexpression of phospholipid hydroperoxide glutathione peroxidase in a human endothelial cell line, *Biochem. J.* 328 (1997) 199–203.
- [44] L. Hori, D. Hatfield, F. Maldarelli, B.J. Lee, K.A. Clouse, Selenium supplementation suppresses tumor necrosis factor α -induced human immunodeficiency virus type 1 replication in vitro, *AIDS Res. Hum. Retroviruses* 13 (1997) 1325–1332.
- [45] C. Sappey, S. Legrand-Poels, M. Best-Belpomme, A. Favier, B. Rentier, J. Piette, Stimulation of glutathione peroxidase activity decreases HIV type 1 activation after oxidative stress, *AIDS Res. Hum. Retroviruses* 10 (1994) 1451–1461.
- [46] A. Gallegos, M. Berggren, J. Gasdaska, G. Powis, Mechanisms of the regulation of thioredoxin reductase activity in cancer cells by the chemopreventive agent selenium, *Cancer Res.* 57 (1997) 4965–4970.
- [47] K.B. Hadley, R.A. Sunde, Selenium regulation of thioredoxin reductase activity and mRNA levels in rat liver, *J. Nutr. Biochem.* 12 (2001) 693–702.
- [48] K. Hirota, M. Murata, Y. Sachi, H. Nakamura, J. Takeuchi, K. Mori, J. Yodoi, Distinct roles of thioredoxin in the cytoplasm and in the nucleus. A two-step mechanism of redox regulation of transcription factor NF-kappa B, *J. Biol. Chem.* 274 (1999) 27891–27897.
- [49] Y. Liu, W. Min, Thioredoxin promotes ASK1 ubiquitination and degradation to inhibit ASK1-mediated apoptosis in a redox activity-independent manner, *Circ. Res.* 90 (2002) 1259–1266.
- [50] T. Tanaka, H. Nakamura, A. Nishiyama, F. Hosoi, H. Masutani, H. Wada, J. Yodoi, Redox regulation by thioredoxin superfamily; protection against oxidative stress and aging, *Free Radic. Res.* 33 (2000) 851–855.
- [51] E.S.J. Arner, A. Holmgren, Physiological functions of thioredoxin and thioredoxin reductase, *Eur. J. Biochem.* 267 (2000) 6102–6109.
- [52] G. Powis, D. Mustacich, A. Coon, The role of the redox protein thioredoxin in cell growth and cancer, *Free Radic. Biol. Med.* 29 (2000) 312–322.
- [53] J.R. Matthews, N. Wakasugi, J. Virelizier, J. Yodoi, R.T. Hay, Thioredoxin regulates the DNA binding activity of NF- κ B by reduction of a disulphide bond involving cysteine 62, *Nucleic Acids Res.* 20 (1992) 3821–3830.
- [54] A.K. Kenworthy, Imaging protein–protein interactions using fluorescence resonance energy transfer microscopy, *Methods* 24 (2001) 289–296.
- [55] F.S. Wouters, P.J. Verveer, P.I.H. Bastiaens, Imaging biochemistry inside cells, *Trends Cell Biol.* 11 (2001) 203–211.

- [56] K. Hirota, M. Matsui, S. Iwata, A. Nishiyama, K. Mori, J. Yodoi, AP-1 transcriptional activity is regulated by a direct association between thioredoxin and Ref-1, PNAS 94 (1997) 3633–3638.
- [57] M. Bjornstedt, S. Kumar, L. Bjorkhem, G. Spyrou, A. Holmgren, Selenium and the thioredoxin and glutaredoxin systems, Biomed. Environ. Sci. 10 (1997) 271–279.
- [58] M. Saitoh, H. Nishitoh, M. Fujii, K. Takeda, K. Tobiume, Y. Sawada, M. Kawabata, K. Miyazono, H. Ichijo, Mammalian thioredoxin is a direct inhibitor of apoptosis signal-regulating kinase (ASK) 1, EMBO J. 17 (1998) 2596–2606.
- [59] R. Geleziunas, W. Xu, K. Takeda, H. Ichijo, W.C. Greene, HIV-1 Nef inhibits ASK1-dependent death signalling providing a potential mechanism for protecting the infected host cell, Nature 410 (2001) 834–838.
- [60] Y. Li, G. Mak, B. Franza Jr., In vitro study of functional involvement of Spl, NF-kappa B/Rel, and API in phorbol 12-myristate 13-acetate-mediated HIV-1 long terminal repeat activation, J. Biol. Chem. 269 (1994) 30616–30619.
- [61] A. Varin, S.K. Manna, V. Quivy, A.-Z. Decrion, C. Van Lint, G. Herbein, B.B. Aggarwal, Exogenous Nef protein activates NF-kappa B, AP-1, and c-Jun N-terminal kinase and stimulates HIV transcription in promonocytic cells. Role in AIDS pathogenesis, J. Biol. Chem. 278 (2003) 2219–2227.
- [62] V.N. Gladyshev, M. Krause, X.-M. Xu, K.V. Korotkov, G.V. Kryukov, Q.-A. Sun, B.J. Lee, J.C. Wootton, D.L. Hatfield, Selenocysteine-containing thioredoxin reductase in *C. elegans*, Biochem. Biophys. Res. Commun. 259 (1999) 244–249.
- [63] T.G. Senkevich, J.J. Bugert, J.R. Sisler, E.V. Koonin, G. Darai, B. Moss, Genome sequence of a human tumorigenic poxvirus: prediction of specific host response-evasion genes, Science 273 (1996) 813–816.
- [64] J.L. Shisler, T.G. Senkevich, M.J. Berry, B. Moss, Ultraviolet-induced cell death blocked by a selenoprotein from a human dermatotropic poxvirus, Science 279 (1998) 102–105.
- [65] L. Zhao, A.G. Cox, J.A. Ruzicka, A.A. Bhat, W. Zhang, E.W. Taylor, Molecular modeling and in vitro activity of an HIV-1-encoded glutathione peroxidase, Proc. Natl. Acad. Sci. U.S.A. 97 (2000) 6356–6361.
- [66] I. Cohen, P. Boya, L. Zhao, D. Metivier, K. Andreau, J.-L. Perfettini, J.G. Weaver, A. Badley, E.W. Taylor, G. Kroemer, Anti-apoptotic activity of the glutathione peroxidase homologue encoded by HIV-1, Apoptosis 9 (2004) 181–192.
- [67] V.N. Gladyshev, T.C. Stadtman, D.L. Hatfield, K.-T. Jeang, Levels of major selenoproteins in T cells decrease during HIV infection and low molecular mass selenium compounds increase, PNAS 96 (1999) 835–839.